JOURNAL OF COMPUTATIONAL PHYSICS 66, 445–457 (1986)

Comparison of Two-Dimensional and Three-Dimensional MHD Equilibrium and Stability Codes

F. HERRNEGGER AND P. MERKEL

Max-Planck-Institut für Plasmaphysik, Garching, Federal Republic of Germany

AND

J. L. JOHNSON*

Plasma Physics Laboratory, Princeton University, Princeton, New Jersey 08544

Received September 13, 1985; revised January 22, 1986

DEDICATED TO THE MEMORY OF RAYMOND C. GRIMM

Stability results obtained with the fully three-dimensional magnetohydrodynamic code BETA, the helically invariant code HERA, and the asymptotic stellarator expansion code STEP agree well for a straight $l=2$, $M=5$ stellarator model. This good agreement between the BETA and STEP codes persists as toroidal curvature is introduced. This validation provides justification for confidence in work with these models.

I. INTRODUCTION

The recent development of stellarators, including the Wendelstein VII-A, Heliotron E, ATF-1, and Wendelstein VII-AS configurations, has renewed interest in the ideal MHD equilibrium and stability properties of configurations having no symmetry. Most of the studies have utilized a reduced set of equations such as the stellarator expansion procedure STEP [1, 2] or three-dimensional codes such as BETA [3]. Some effort has been made to validate these codes. Good agreement has been found [1, 4] between the equilibrium predictions obtained with the stellarator expansion and those from three-dimensional models. Similarly, stability predictions obtained for a straight helical system with the BETA code agree well [5] with those from the helically invariant HERA code [6]. The purpose of this paper is to continue this validation process by comparing the stability predictions of the stellarator expansion method with those of Ref. [5] for a straight $l=2$ stellarator and to those of the BETA code as toroidal curvature is introduced. This is one of the few cases where, on the basis of a mode analysis, a comparison of the predictions of the

* On loan from Westinghouse Research and Development Center, Pittsburgh, Pennsylvania.

0021-9991/86 $3.00

stability properties of a truly three-dimensional system by different computational methods has been made.

We describe our model in Section II and report a few results for straight $l=2$ systems in Section III. We obtain good agreement between the predictions of the three codes for fixed-boundary modes and of the STEP and HERA codes for free-boundary modes. In Section IV we introduce toroidal curvature into the model by continuously bending the straight system. Here we obtain good agreement between STEP and BETA for fixed-boundary computations. We summarize our results in Section V and make a few observations.

II. Model

It is difficult to make this kind of comparison because of differences in specifications of the equilibrium parameters. In all three codes we consider a straight $l=2$ field configuration of length $L=ML_p$ with $M=5$ field periods of length L_p and pitch $ha=2\pi a/L_p=0.66$. For the BETA code [3] we prescribe an elliptically shaped plasma boundary of average radius a with the ellipticity Δ_2 chosen to obtain the desired vacuum-field rotational transform or twist at the magnetic axis. We vary the average beta, $\langle\beta\rangle \approx 2\langle p\rangle/B_0^2$, with B_0 the main magnetic field, keeping the ellipticity fixed and maintaining zero net current on each magnetic surface. We assume a pressure profile $p=p_0[1-(r/a)^2]$ with the surface label r the average radius. The pressure varies linearly with the area enclosed by the magnetic surfaces. The density distribution used to normalize the eigenvalue is given by $\rho(r)=[p(r)/p_0]^{1/2}$. We use $(\gamma L/2\pi v_A)^2$ as our eigenvalue, with v_A the Alfvén velocity at the magnetic axis. The relation $(L/2\pi a)(\gamma a/v_A)_{\mathrm{BETA,HERA}} = (\gamma L/2\pi v_A)$ is used to convert the normalized eigenvalues in Ref. [5] to those of the present paper. The equilibrium configuration is unstable if the eigenvalue is negative. The HERA model [6] is similar. These models are described in Ref. [5].

In the work with STEP [1, 2], we use an r, θ, z pseudocylindrical coordinate system. We prescribe a vacuum field

$$B=B_0\left[\mathbf{e}_z+\frac{\delta}{h}\nabla I_2(hr)\sin(2\theta-hz)+\cdots\right], \tag{1}$$

with the Bessel function $I_2(hr)$ a solution of Laplace's equation in a straight system and the parameter δ chosen to obtain the desired twist ι_0 on axis. This is the model that was used in the early stellarator studies [7]. In the long pitch limit, $ha<1$, the rotational transform varies as

$$\iota(r)=\iota_0\left[1+\frac{1}{2}(hr)^2+\frac{7}{96}(hr)^4+\cdots\right] \tag{2}$$

with $\iota = M\delta^2/16$. In the STEP model the pressure varies as $p = p_0(1 - \Psi)$ with Ψ the normalized poloidal flux inside a magnetic surface. We do not change the helical field as we introduce toroidicity, changing only the metric element associated with the coordinate z and keeping the same helical pitch and number of field periods. As we change the toroidal curvature, we adjust the vertical field to keep the plasma approximately centered.

In the BETA code [3], we study the stability properties by repeating the energy minimization of the equilibrium study subject to an additional constraint and extrapolate in the grid size. This results in a problem of determining differences between large terms. In both the STEP [2] and HERA [6] codes, we formally extremize the Lagrangian associated with small perturbations from equilibrium. In STEP, the lowest order displacement vector is given in terms of a stream function η, such that

$$\xi = \nabla z \times \nabla \sum_m \eta_m[\Psi^{(0)}] \exp i(m\theta - 2\pi n z/L). \tag{3}$$

The numbers m and n represent the poloidal and toroidal mode numbers. In our plots we present only this lowest order displacement, based on axisymmetric lowest order flux surfaces. This simplification removes much of the complication associated with the actual eigenfunction and makes interpretation of the results easier. We restrict the rotational transform to values near $\iota \approx 0.5$ in all of our studies. Since Fourier modes with different m-numbers decouple in straight systems, the $m = 2$, $n = 1$ instability is the only mode of concern. Neighboring poloidal components become important as toroidicity is introduced.

Instabilities where a conducting wall is placed outside the plasma, or even infinitely far away, can be studied easily with both the STEP and HERA codes. We typically introduce a perfectly conducting surface with the same shape as the plasma boundary but with a mean minor radius b. In principle, these free-boundary modes can also be investigated with BETA, but much effort is needed to get accurate results. We did not use BETA for free-boundary modes in this study.

Calculations with several computational grids and extrapolation to infinite mesh should be done with all three codes. We find that this is essential for both the BETA and HERA codes. However, in the work with STEP, the results obtained with reasonably sized grids (128 azimuthal and 96 surface points for constructing the Fourier components of the equilibrium properties, 48 radial expansion functions, and 20 spectral components) are so close to what is obtained from the extrapolation that the extra effort is not necessary.

III. Straight Systems

We consider a class of equilibria with a fixed value of $\langle \beta \rangle$ and different values of the rotational transform at the magnetic axis. Results for fixed-boundary modes in

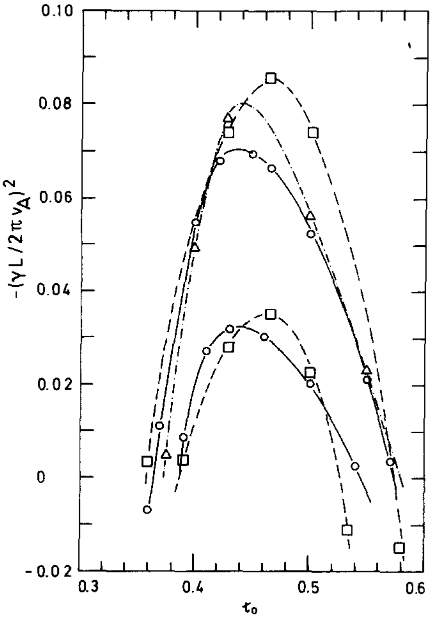

FIG. 1. Eigenvalue $(\gamma L/2\pi v_A)^2$ as a function of the twist ι_0 at the magnetic axis for fixed-boundary $m=2$, $n=1$ modes in a straight stellarator. The triangles refer to results from HERA, the squares from BETA, and the circles from STEP. The upper curves are for $\langle\beta\rangle = 3\%$; the lower ones are for $\langle\beta\rangle = 1.5\%$.

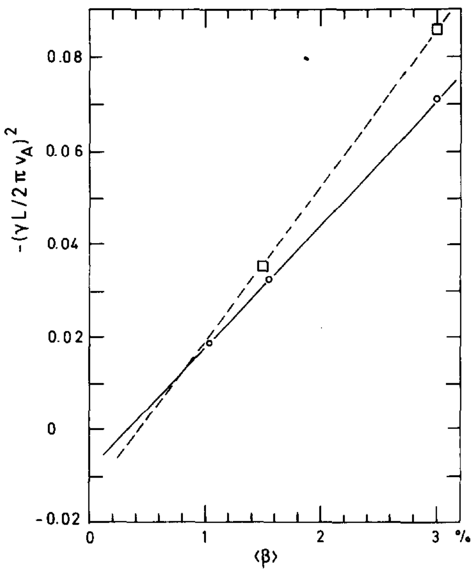

FIG. 2. Maximum eigenvalue $(\gamma L/2\pi v_A)^2$ as a function of $\langle\beta\rangle$ for fixed-boundary modes in a straight system. The squares refer to results from BETA and the circles from STEP. This leads to an estimate of the critical beta; $\langle\beta\rangle_c \approx 0.3\%$.

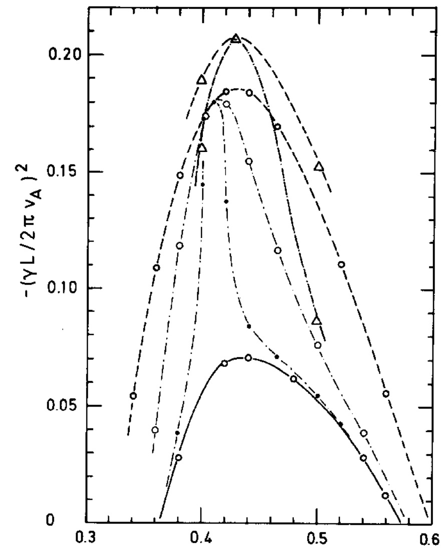

FIG. 3. Eigenvalue $(\gamma L/2\pi v_A)^2$ as a function of ι for $\langle\beta\rangle = 3.0\%$ at several wall positions. The triangles refer to results from HERA and the circles and dots from STEP. The solid curve is for a fixed-boundary case where a conducting shell is placed at the plasma surface. The dashed curves are for a free-boundary mode with the wall infinitely far out. The broken curves have intermediate walls of radius b with $b/a = 1.1$. The dotted curve, from STEP, has b/a 1.001.

systems with $\langle\beta\rangle = 1.5\%$, corresponding to $\beta(0) = 0.030$, and $\langle\beta\rangle = 3.0\%$ $[\beta(0) = 0.058]$ are shown in Fig. 1. The maximum of the eigenvalue curve for STEP occurs near where the boundary twist is $\iota_a = 0.5$. Similar runs with different density distributions and for other values of $\langle\beta\rangle$ also show good agreement.

A slightly different comparison is given in Fig. 2. Here we plot the maximum value of the eigenvalue curve for a given $\langle\beta\rangle$-value as a function of $\langle\beta\rangle$ obtained

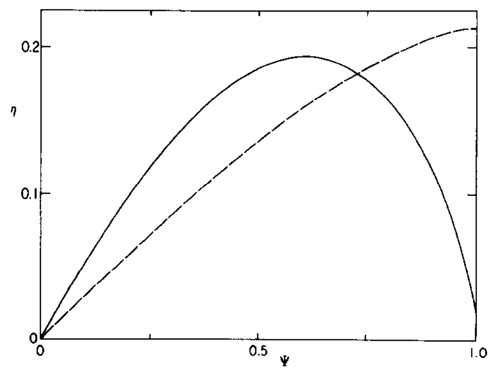

FIG. 4. Eigenfunction η for fixed-boundary (solid curve) and close-fitting wall ($b/a = 1.001$, broken curve) modes of Fig. 3 at $\iota_0 \approx 0.4084$ $(\iota_a = 0.5]$, as obtained with STEP.

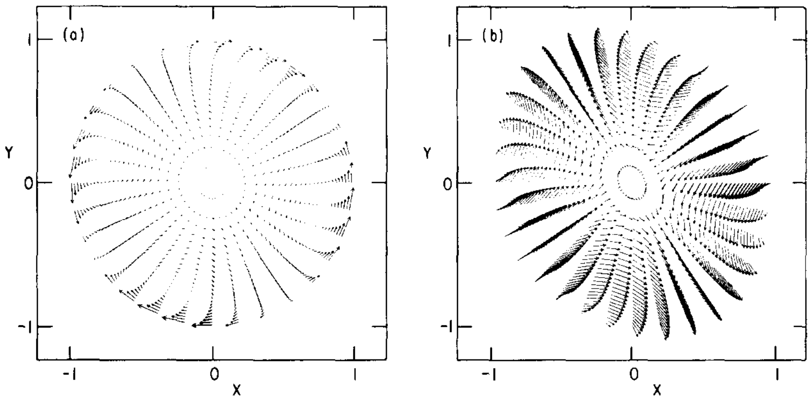

FIG. 5. Displacement vectors associated with the modes of Fig. 4. (a) Fixed-boundary, (b) $b/a = 1.001$.

with the STEP and BETA codes. The maxima occur at slightly different values of ι_0 for the two codes. It is useful to note that the predicted critical $\langle\beta\rangle$'s at which this $m = 2$ mode is marginal are nearly the same.

We give in Fig. 3 the eigenvalue as a function of ι_0 for $\langle\beta\rangle = 3\%$ at several positions b/a of an external conducting wall in order to investigate the effect of relaxing the boundary condition at the plasma surface. Again, good agreement is obtained from the STEP and HERA codes.

It can be seen from Fig. 3 that the eigenvalue is very nearly the same for the fixed-boundary case as it is for the free-boundary one where the wall is close to the

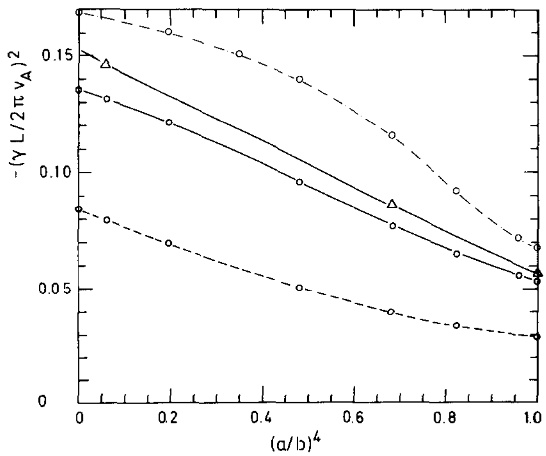

FIG. 6. $(\gamma L/2\pi v_A)^2$ versus $(a/b)^4$ for $\langle\beta\rangle = 3.0\%$. The solid curves are for $\iota_0 = 0.50$, the dashed curve for $\iota_0 = 0.54$, the broken curve for $\iota_0 = 0.4$. The circles refer to results from STEP and the triangles from HERA.

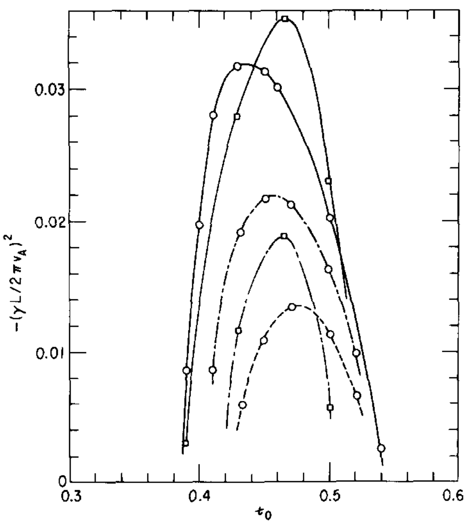

FIG. 7. $(\gamma L/2\pi v_A)^2$ as a function of ι_0 for $\langle\beta\rangle = 1.5\%$. The squares refer to results from BETA, the circles from STEP. The solid curves are for a straight system with $L/2\pi R = 0$; the broken curves are for $L/2\pi R = 0.5$ with a vertical field $B_v/B_0 = 0.009$ to center the discharge; the dashed curve is for $L/2\pi R = 0.7$.

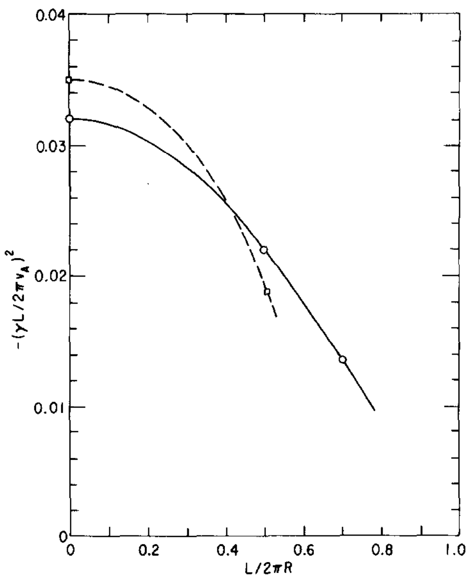

FIG. 8. Maxima of the eigenvalue curves of Fig. 7 at constant $\langle\beta\rangle$ versus $L/2\pi R$. The squares refer to results from BETA, the circles from STEP. These lead to stability before $L/2\pi R = 1$.

plasma, except near $\iota_0 \approx 0.4084$. There the free-boundary eigenvalue approaches that of a free-boundary mode with the wall far outside. The explanation for this behavior is that the rotational transform at the plasma surface approaches the resonance value $\iota = 0.5$ for $n/m = \frac{1}{2}$ so that the normal component of the perturbed field, $\delta B_{\Psi} = (B_0/a)(m\iota - n)\,\xi_{\Psi}$, is zero for any finite value of the displacement vector. Thus incorporation of a free-boundary model relaxes the fixed-boundary condition that $\xi_{\Psi}(a) = 0$ without introducing any stabilizing energy from the vacuum region. The difference in the perturbations can be seen in Figs. 4 and 5 where the stream function $\eta(\Psi)$ and the displacement vector ξ are given for the fixed-boundary and $b/a = 1.001$ cases. This resonance phenomenon at rational values of ι is very pronounced for the STEP calculations in a straight system where the lowest order flux surfaces are functions of only one variable, $\Psi^{(0)} = \Psi^{(0)}(r)$. In such a case, modes with different m numbers decouple. It is less apparent in calculations where toroidicity is introduced [8]. In these cases the equilibrium properties depend on

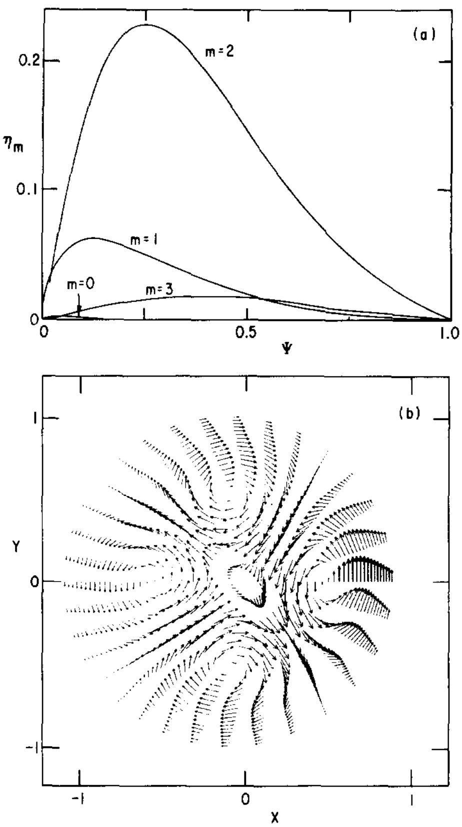

FIG. 9. Eigenfunction η and displacement vector ξ from STEP for the fixed-boundary mode of Fig. 7 with $\langle\beta\rangle = 1.5\%$, $L/2\pi R = 0.7$, $B_v/B_0 = 0.009$, and $\iota_0 = 0.5$; $(\gamma L/2\pi v_A)^2 = -0.014$.

two variables and the different poloidal Fourier modes are coupled. When this happens, the mixing of the poloidal Fourier harmonics provides stabilization and reduces the effect of the resonance.

The stabilizing effect of a conducting wall on free-boundary modes is shown in Fig. 6. Plots of the eigenvalue as a function of a/b show that γ^2 scales as $(a/b)^4$, except for modes exhibiting resonance. This agrees well with analytical expectations [7], which are that the perturbation in the outside region varies as $(r/a)^{-2m}$. Similar plots of the eigenvalue as a function of other equilibrium parameters lead to the scaling relation $-(\gamma a/v_A)^2 \sim \langle\beta\rangle(ha)^2(\iota_0/M)$ which was obtained previously [9].

IV. Toroidal Systems

In the comparison of the STEP and BETA codes when toroidal curvature is present, we consider a class of equilibria with $\langle\beta\rangle = 1.5\%$. Eigenvalues as functions

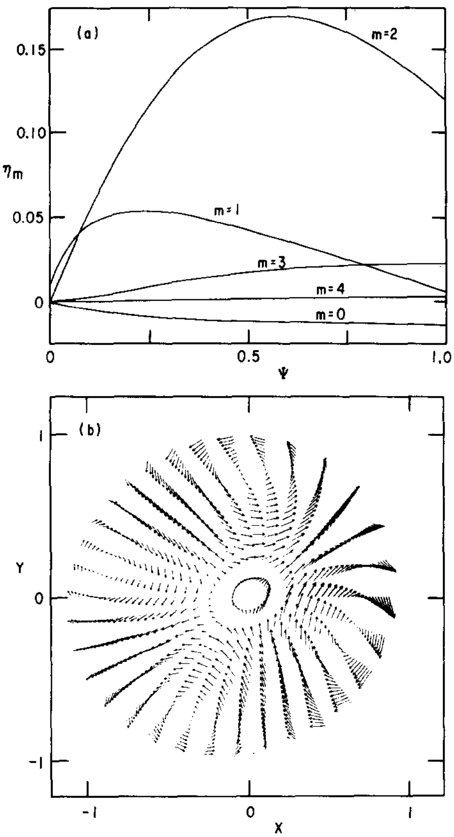

Fig. 10. Eigenfunction η and displacement vector ξ from STEP for a free-boundary mode in a system with $\langle\beta\rangle = 1.5\%$, $L/2\pi R = 0.7$, $B_v/B_0 = 0.009$, and $\iota_0 = 0.5$; $(\gamma L/2\pi v_A)^2 = -0.049$.

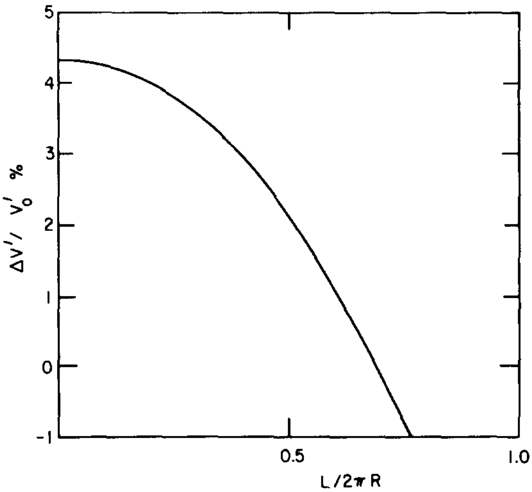

FIG. 11. $\Delta V'(\Phi)/V'_0$ as a function of $L/2\pi R$ for equilibria with $\langle\beta\rangle = 1.5\%$ and ι_0 chosen to maximize the eigenvalue. Here Φ is the toroidal flux, and the change in $V'(\Phi)$ associated with diamagnetic current has been omitted so that the slope measures the part of the average magnetic well that provides stabilization. The vertical field is varied as $B_v/B_0 \sim (L/2\pi R)^{1/2}$.

of ι_0 are given in Fig. 7 for several values of $L/2\pi R$ with R/a the toroidal aspect ratio. As noted earlier, the toroidal curvature has no relation to the length of a field period L_p in our model. The periodicity length L imposed on the perturbation is the same five-period length that was used for the straight system. Again, if we determine the maxima of the eigenvalue curves as functions of ι_0 at constant $L/2\pi R$ and plot these maximum eigenvalues for different values of $L/2\pi R$ as in Fig. 8, we obtain satisfactory agreement between the two codes. Both codes show the stabilizing effect of toroidal curvature. The system becomes stable with respect to an $m=2$, $n=1$ mode for this $\langle\beta\rangle$ before the five-field-period length closes on itself. The stabilizing effect of toroidal curvature on free-boundary modes is discussed in Ref. [8]. As curvature is introduced, the unstable eigenfunctions lose their pure $m=2$ Fourier character as can be seen in the fixed-boundary instability plots of Fig. 9 and the analogous free-boundary modes of Fig. 10.

The stabilizing effect of toroidal curvature can be explained by the average magnetic well created by the outward shift of the magnetic axis associated with the Pfirsch-Schlüter current. This is illustrated in Fig. 11, where the well depth $\Delta V'/V$ is plotted as a function of the toroidal curvature parameter $L/2\pi R$. This was calculated using the STEP code.

V. DISCUSSION

The quantitative agreement between the results of the different codes are better than might have been expected. All three have reason for confidence when used for properly chosen applications. The HERA treatment of the equilibrium and stability properties of a helically invariant system should be expected to be quite accurate since the code uses the formalism developed in the ERATO code for axially symmetric configurations [10]. Since the BETA code uses an energy minimizing technique to get to an equilibrium configuration, it is reasonable to expect it to provide good equilibrium properties. Although its stability predictions should be less reliable since they are determined from a calculation requiring cancellation of large terms in the energy, they too should give some insight. The STEP program is based on the smallness of the ratio of the helical field to the toroidal field at the plasma boundary, which for a typical case in this paper is about 0.2. Even though the model consists of averaging over the helical field periods as if there were an infinite number, the smallness of B_δ/B_0 gives considerable hope that the results can give some insight into the physics. Since the STEP code uses the formulation developed in the PEST program for equilibrium and stability studies of axisymmetric configurations [11], it should give reliable results. Thus, although the asymptotic expansion methods used in STEP could have some effect, the principal difference in results is due to the difficulty involved in representing the same equilibrium configuration because of the different ways of specifying the boundary shapes and pressure distributions. The good agreement found in this work indicates that the global instabilities do not depend strongly on the exact specification of plasma shape or pressure distribution for this model stellarator.

This work provides considerable justification for using asymptotic methods such as STEP [1, 2] or an analogous specific variable approximation [12], stellarator expansion initial value codes [4, 13], helical-axis modifications of this expansion [14, 15], or other numerical techniques [16] to get a rough understanding of the MHD properties of a stellarator configuration, and then use the more powerful three-dimensional techniques to refine the work. Some progress in this direction has already been made, including prediction of a possible Pfirsch–Schlüter-current-driven instability in the ATF-1 device [17], with correction possible by adjusting the external vertical field with increasing $\langle\beta\rangle$ [18], and estimations of unstable free-boundary mode eigenvalues in Wendelstein VII-A and more compact $l=2$ stellarators [8].

An interesting physics result that was made obvious in this study was the difference in behavior of unstable fixed-boundary modes from free-boundary modes in a one-dimensional plasma model where the rotational transform has low-order rationality at the plasma surface (as in Fig. 3). This arises because the perturbed magnetic field becomes small at the plasma surface, no matter what the displacement vector does. Thus the usual constraint on the perturbation is relaxed. Although this effect is not as pronounced when the mode separation is less complete, this mechanism may provide a partial explanation for the strong deterioration of energy confinement in Wendelstein VII-A as the twist is varied through these rational values. Since there is little shear in this device, a possibly more plausible explanation would be the loss of equilibrium when the magnetic field lines close on themselves.

If the toroidal curvature is increased beyond a critical value in our model, the $m = 2$ mode becomes stable. This occurs before the five-field-period magnetic structure closes on itself. As indicated by the variation of $\Delta V'/V'_0$ in Fig. 11, this is associated with the outward shift of the magnetic surfaces with respect to the plasma boundary which creates a sufficiently strong magnetic well to provide stabilization. Another estimate of the effect of curvature on the stability properties is given by the Mercier criterion [19] which measures the interaction of shear with both the normal curvature (which creates the average magnetic well) and the geodesic curvature. Although both the $\Delta V'/V'_0$ and Mercier criteria are derived by considering high m and n localized modes or shearless systems, they provide some indication of the stability properties with respect to low-m modes for systems with little force-free current. It has been shown in other studies that the Pfirsch–Schlüter current can drive kink like modes even though there is no net force-free current in the plasma at sufficiently large values of beta [17]. As discussed in a recent study of Mercier and ballooning mode criteria [20], the stabilization associated with the deepening of the magnetic well because of the Pfirsch–Schlüter current competes with the destabilizing forces associated with these currents. More work should be done to resolve these relationships, particularly with respect to higher-n modes.

ACKNOWLEDGMENTS

We dedicate this paper to the memory of Dr. R. C. Grimm, the principal architect of the PEST program. He would have appreciated this study of the comparison of the results of different numerical approaches and the resultant validation of these codes. We are indebted to Dr. A. Schlüter and Dr. J. Nührenberg for encouraging our work on this problem. Several useful discussions with members of the IPP Theorie 2 Division and the PPL theory group deserve grateful acknowledgment. One of us (J.L.J.) was supported by the U. S. Department of Energy Contract DE-AC02-76-CHO-3073 with Princeton University. He appreciates the kindness of Dr. P. H. Rutherford and Dr. F. W. Perkins, and the hospitality of IPP, Garching for a visit when this effort was formulated and started.

REFERENCES

1. G. ANANIA, J. L. JOHNSON, AND K. E. WEIMER, *Phys. Fluids* **26**, 2210 (1983).
2. G. ANANIA AND J. L. JOHNSON, *Phys. Fluids* **26**, 3070 (1983).
3. F. BAUER, O. BETANCOURT, AND P. GARABEDIAN, *Magnetohydrodynamic Equilibrium and Stability of Stellarators* (Springer-Verlag, New York 1984).
4. B. A. CARRERAS, H. R. HICKS, J. A. HOLMES, V. E. LYNCH, L. GARCIA, J. H. HARRIS, T. C. HENDER, AND B. F. MASDEN, *Phys. Fluids* **26**, 3569 (1983).
5. O. BETANCOURT, F. HERRNEGGER, P. MERKEL, AND J. NÜHRENBERG, *J. Comput. Phys.* **52**, 187 (1983).
6. R. GRUBER, S. SEMENZATO, F. TROYON, T. TSUNEMATSU, W. KERNER, P. MERKEL, AND W. SCHNEIDER, *Comput. Phys. Comm.* **24**, 363 (1981).
7. J. L. JOHNSON, C. R. OBERMAN, R. M. KULSRUD, AND E. A. FRIEMAN, *Phys. Fluids* **1**, 281 (1958).
8. F. HERRNEGGER AND J. L. JOHNSON, in *Twelth European Conference on Controlled Fusion and Plasma Physics, Budapest, 1985*, edited by L. Pòcs and A. Montvai (European Physical Society, Budapest, 1985), Part 1, p. 409.
9. J. P. FREIDBERG, *Phys. Fluids* **16**, 1349 (1973).

10. R. GRUBER, F. TROYON, D. BERGER, L. C. BERNARD, S. ROUSSET, R. SCHREIBER, W. KERNER, W. SCHNEIDER, AND K. V. ROBERTS, *Comput. Phys. Comm.* **21**, 323 (1981).
11. R. C. GRIMM, J. M. GREENE, AND J. L. JOHNSON, in *Methods in Computational Physics*, edited by J. Killeen (Academic Press, New York, 1976), Vol. 16, p. 253.
12. V. D. PUSTOVITOV, V. D. SHAFRANOV, L. E. ZAKHAROV, L. M. DEGTYAREV, V. V. DROZDOV, S. YU. MEDVEDEV, YU. YU. POSHEKHONOV, AND M. I. MIKHAIJLEV, in *Plasma Physics and Controlled Nuclear Fusion Research, 1982* (International Atomic Energy Agency, Vienna, 1983), Vol. II, p. 541.
13. H. R. STRAUSS AND D. A. MONTICELLO, *Phys. Fluids* **24**, 1148 (1981).
14. A. E. KONIGES AND J. L. JOHNSON, *Phys. Fluids* **28**, 3127 (1985).
15. T. C. HENDER AND B. A. CARRERAS, *Phys. Fluids* **27**, 2101 (1984).
16. R. CHODURA, R. GRUBER, F. HERRNEGGER W. KERNER, W. SCHNEIDER, AND F. TROYON, in *Plasma Physics and Controlled Nuclear Fusion Research, 1980* (International Atomic Energy Agency, Vienna, 1981), Vol. 1, p. 813.
17. G. REWOLDT AND J. L. JOHNSON, *Nucl. Fusion* **24**, 733 (1984).
18. B. A. CARRERAS, H. R. HICKS, J. A. HOLMES, V. E. LYNCH, AND G. H. NEILSON, *Nucl. Fusion* **24**, 1347 (1984).
19. J. M. GREENE AND J. L. JOHNSON, *Plasma Phys.* **10**, 729 (1968).
20. J. NÜHRENBERG AND R. ZILLE, in *Twelth European Conference on Controlled Fusion and Plasma Physics, Budapest, 1985*, edited by L. Pòcs and A. Montvai (European Physical Society, Budapest, 1985), Part 1, p. 445.